

Formation of the reactive interface AlSb/Sb(111) investigated by high-resolution electron-energy-loss spectroscopy

J.-L. Guyaux, R. Sporcken, P. A. Thiry, and R. Caudano

Laboratoire Interdisciplinaire de Spectroscopie Electronique, Institute for Study in Interface Sciences, Facultés Universitaires Notre-Dame de la Paix, 61 rue de Bruxelles, B-5000 Namur, Belgium

Ph. Lambin

Laboratoire de Physique du Solide, Institute for Study in Interface Sciences, Facultés Universitaires Notre-Dame de la Paix, 61 rue de Bruxelles, B-5000 Namur, Belgium

L. Patry and D. Roy

Département de Physique, Université Laval, Québec, Canada G1K 7P4

(Received 27 September 1993)

The reaction of Al deposited on Sb(111) was studied by high-resolution electron-energy-loss spectroscopy. The formation of AlSb was confirmed by the observation of the surface optical phonon of the compound at 332 cm^{-1} (41 meV). A quantitative interpretation of the AlSb/Sb interface formation is proposed, based on the dielectric theory of electron-energy-loss spectroscopy.

I. INTRODUCTION

Heterostructures play a key role in microelectronics development, especially the ones involving semiconductor/semiconductor interfaces. In the past decades, less attention has been paid to semimetal-semiconductor superlattices. Such heterostructures are indeed expected to show unique properties such as a transition of the buried semimetal into a narrow-band-gap semiconductor.¹ These systems can be very attractive for detectors working in the infrared. However, before being able to grow such complex multilayers, it is of great importance to study simple systems such as a single semiconductor/semimetal interface. As an example, the formation of the AlSb/Sb(111) interface has already been studied by x-ray photoelectron spectroscopy (XPS), Auger-electron spectroscopy (AES), and low-energy electron diffraction (LEED) and photoemission induced by synchrotron radiation.² When aluminum was deposited on a substrate held at room temperature, the appearance of reacted AlSb species was observed first, immediately followed by the growth of metallic Al islands. When the deposition was performed on a heated substrate (600 K) no significant excess of metallic Al could be detected at the surface and epitaxial growth of AlSb was indicated by LEED.³ This observation is further confirmed by the high-resolution electron-energy-loss spectroscopy (HREELS) measurements discussed in the present paper.

HREELS has often been used to study the chemical and structural modifications induced at the surface by the reaction with foreign atoms or molecules. This technique has demonstrated a remarkable sensitivity permitting fractions of monolayer coverage to be detected, often exceeding the sensitivity of spectroscopies such as XPS and AES. One of the merits of HREELS is its high sensitivity to light elements like hydrogen.

In HREELS, elemental identification always occurs in-

directly, mostly through the observation of molecular vibrations of adsorbed or reacted species at the surface of the sample. In some cases, the reaction produces a chemical compound that can be identified unambiguously from its surface optical-phonon fingerprint. These phonons are similar to the modes described by Fuchs and Kliever⁴ for an ionic slab. They have been observed by HREELS in many infrared-active materials. Let us only mention here the pioneering work of Ibach on ZnO (Ref. 5) and the more recent results obtained on insulators samples thanks to the use of a neutralization electron gun.⁶

In the experiment described here, HREELS serves to fingerprint the formation of a reacted layer at the interface between aluminum and antimony. Here the observation of energy losses characteristic of AlSb provides evidence for the formation of that compound on the Sb single crystal. Although numerous HREELS spectra have already been published for III-V semiconductors like GaAs,⁷ Al_xGa_{1-x}As,⁸ InP,⁹ InSb,¹⁰ InAs,¹¹ and GaSb,¹¹ no such measurements on AlSb single crystal have been reported in the literature so far. The likely reason is that AlSb single crystals are difficult to make and to keep unaltered in air because of the higher affinity of aluminum toward oxygen and water vapor than toward antimony. Nevertheless, infrared measurements have been performed on an AlSb single crystal from which we are able to estimate the frequency of the Fuchs-Kliever (FK) surface phonon of AlSb, useful for interpreting our HREELS measurements. Due to its cubic zinc-blende structure, the infrared spectrum of AlSb involves only one lattice oscillator corresponding to opposite displacements of the Al and Sb fcc sublattices. Neglecting the damping factor, i.e., assuming an infinite lifetime for the vibration, the frequency of the surface phonon is estimated by $\omega_{\text{FK}} = \omega_{\text{TO}} \sqrt{[\epsilon(0)+1]/[\epsilon(\infty)+1]}$ where $\epsilon(0)$ and $\epsilon(\infty)$ are the static and high-frequency dielectric constants of AlSb and ω_{TO} is the frequency of the transverse

TABLE I. Infrared optical constants of AlSb taken from Ref. 16, except for the ω_{TO} frequency, which has been adjusted to the experimental loss spectrum. The ω_{LO} followed from the Lyddane-Sachs-Teller relation. The plasma frequency and the damping parameter of antimony are listed in the last line.

	ω_{TO} (cm^{-1})	ω_{LO} (cm^{-1})	$\epsilon(0)$	$\epsilon(\infty)$	$\Delta\epsilon$	γ	ω_p (eV)	γ_p
AlSb	315	334	11.11	9.88	1.33	0.006		
Sb				1.0			14.0	0.43

optical phonon at long wavelength. Introducing in that formula the values found in the literature (Ref. 16), one obtains 338 cm^{-1} as a first estimate for the FK mode of AlSb.

The excitation of FK phonons in specular EELS is well described by the dielectric theory of electron-energy-loss spectroscopy. In that context, the energy-loss spectrum is completely determined by the electron impact energy (E_0), the geometry of the experiment, and the infrared dielectric response of the bulk material. This theoretical relationship allows the parameters of the dielectric function to be deduced from the analysis of the HREELS data.

The crystal structure of antimony is rhombohedral. Its (111) plane forms a hexagonal net where the interatomic distance is 4.308 \AA . AlSb crystallizes in the zinc-blende structure where the spacing between two atoms in the (111) hexagonal plane is 4.338 \AA . This results in an in-plane lattice mismatch of 0.6% in the (111) plane. Based on these simple geometrical considerations, one expects that epitaxy could be possible between AlSb and Sb.

The technique used here to grow crystalline AlSb on antimony is similar to molecular-beam epitaxy (MBE) except that only one element, aluminum, is evaporated from a Knudsen cell while the Sb atoms are supplied by interdiffusion from the substrate held at a temperature high enough to avoid any excess of metallic aluminum at the surface. This growth technique has the advantage of being very simple. It permits us to grow thick crystalline films of several hundred \AA and has already been successfully applied to the growth of InSb/Sb (Ref. 12) and more recently GaSb/Sb.¹³

II. EXPERIMENTAL RESULTS

The antimony single crystals were cleaved under an argon flow along the (111) cleavage plane and immediately loaded into the ultrahigh-vacuum (UHV) chamber. The *in situ* cleaning consisted of a gentle Ar^+ sputtering (500 eV , $1 \mu\text{A}/\text{cm}^2$, 10 min) followed by annealing at 550 K . The cleanliness of the surface was checked by LEED, AES, and HREELS. No energy-loss structure is visible on the clean surface (lower spectrum of Fig. 1).

Al was evaporated from a Knudsen cell on the Sb substrate held at 600 K . All depositions were done in a preparation chamber connected to the analysis chamber. Figure 1 displays a series of HREELS spectra recorded after successive Al depositions. The electron impact energy was 6.9 eV and the common angle of incidence and analysis was 45° . The rate of evaporation was monitored

with a quartz crystal oscillator. The Al coverage has been converted in thickness of AlSb uniform layer, one AlSb monolayer being equivalent to $6.136 \times 10^{14} \text{ Al atoms}/\text{cm}^2$ and corresponds to 3.542 \AA .

From the HREELS results shown in Fig. 1, we can state the following.

(i) From the very beginning of the aluminum deposition, an energy-loss peak and its corresponding energy gain are clearly identified at 332 cm^{-1} (41 meV) on both sides of the elastic peak. This energy peak is very close to that predicted above for the FK mode of AlSb (338 cm^{-1}). We can conclude that these peaks testify to the formation of AlSb as they are related to the creation and annihilation of the long-wavelength Fuchs-Kliwer phonon of the compound.

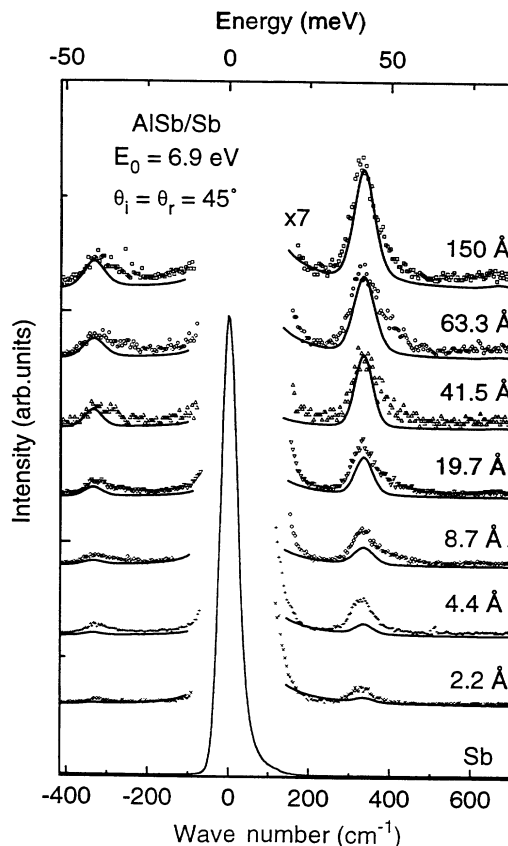


FIG. 1. Synoptic panel showing typical HREELS spectra recorded for increasing Al coverage on Sb(111). The full curves are the results of the theoretical calculation using the dielectric theory with the parameters of Table I.

(ii) The frequency of the surface phonons measured on the spectra does not shift significantly with the aluminum coverage. This indicates that AlSb is formed immediately and no precursor or intermediate bonding state takes place at the early stage of the growth. Most probably, AlSb grows in small islands that gradually coalesce to form a complete layer.

(iii) The increasing intensity ratio between the first energy loss and the elastic peak intensity is strongly dependent on the thickness of AlSb formed on top of the Sb crystal.

III. THEORETICAL ANALYSIS

The theoretical formulation of the dielectric theory applied to a two-layer system has been established in several papers.¹⁴ It is based on an effective dielectric function for the layered system which, in the present case, is an AlSb layer of thickness d on a semi-infinite Sb substrate. The effective dielectric function can be written as

$$\xi(\mathbf{q}_{\parallel}, \omega) = \varepsilon_s(\omega) \frac{\varepsilon_s(\omega) \tanh(q_{\parallel} d) + \varepsilon_b(\omega)}{\varepsilon_b(\omega) \tanh(q_{\parallel} d) + \varepsilon_s(\omega)}, \quad (1)$$

where $\varepsilon_s(\omega)$ and $\varepsilon_b(\omega)$ are the dielectric functions of AlSb and Sb, respectively. In the infrared, $\varepsilon_s(\omega)$ is described by the usual formula

$$\varepsilon_s(\omega) = \varepsilon_s(\infty) + \frac{[\varepsilon_s(0) - \varepsilon_s(\infty)] \omega_{\text{TO}}^2}{\omega_{\text{TO}}^2 - \omega^2 - i \gamma_s \omega_{\text{TO}} \omega}, \quad (2)$$

where ω_{TO} is the frequency of the transverse optical phonon of AlSb, γ_s is an empirical damping factor, and $\varepsilon_s(0)$ and $\varepsilon_s(\infty)$ are the static and the high-frequency dielectric constants.

In Eq. (1), $\varepsilon_b(\omega)$ represents the dielectric function of the Sb substrate. As there are no dipole-active phonons in this semimetallic element, the dielectric function is represented by a Drude term which accounts for free-electron plasma excitations:

$$\varepsilon_b(\omega) = 1 - \frac{\omega_p^2}{\omega^2 - i \gamma_b \omega_p \omega}, \quad (3)$$

where ω_p is the plasma frequency and γ_b is a damping factor.

The surface dielectric response $g(\mathbf{q}_{\parallel}, \omega)$ of the material described by the effective dielectric function $\xi(\mathbf{q}_{\parallel}, \omega)$ is given by

$$g(\mathbf{q}_{\parallel}, \omega) = \frac{\xi(\mathbf{q}_{\parallel}, \omega) - 1}{\xi(\mathbf{q}_{\parallel}, \omega) + 1} \quad (4)$$

from which the dielectric theory makes it possible to calculate the entire energy-loss spectrum. The probability of exciting one optical phonon of energy $\hbar\omega$ is obtained by integrating the product of the imaginary part of $g(\mathbf{q}_{\parallel}, \omega)$ and a kinematic factor in the \mathbf{q} space.¹⁵

The parameters of the dielectric function of the Sb substrate have been measured on the energy-loss spectrum shown in Fig. 2 and obtained at 65 eV on a clean antimony single crystal. From the surface plasmon observed at 8.9 eV (see Fig. 2), one can deduce a value of

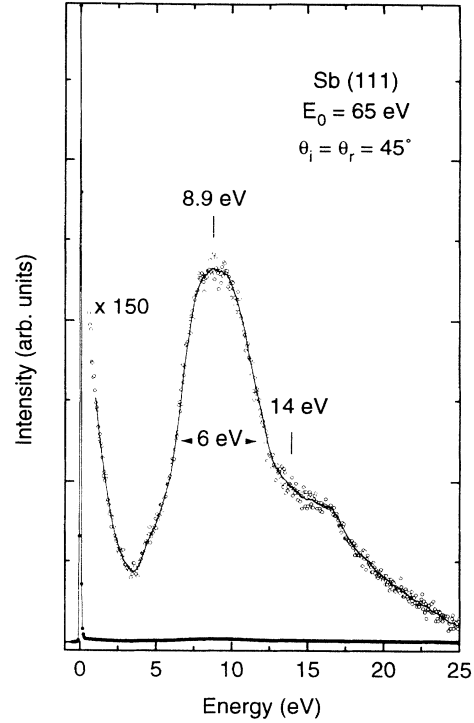


FIG. 2. 65-eV electron-energy-loss spectrum recorded on clean Sb(111). The broad peak located at 8.9 eV is interpreted as a surface plasmon.

$\omega_p = 14.0$ eV for the bulk plasmon. Similarly, the damping factor [Eq. (3)] is estimated from the width (6 eV) of the surface-plasmon loss peak (see Table I).

In order to determine the optical parameters of AlSb, a 1000-Å-thick film was grown on Sb(111). In this case the thickness of the AlSb overlayer is much larger than the wavelength of the surface optical phonons and Eq. (2) can be used to describe the overall response function of the system: i.e., $\xi(\omega, \mathbf{q}_{\parallel}) = \varepsilon_s(\omega)$. A theoretical simulation of the full spectrum was performed with the parameters found in the literature.¹⁶ These parameters yield a FK mode frequency slightly above the measured one. Consequently, we have lowered the resonance frequency ω_{TO} by 4 cm^{-1} so as to reproduce the observed $\omega_{\text{FK}} = 332 \text{ cm}^{-1}$ frequency. Figure 3 shows the computed spectrum superimposed on the experimental one. The parameters used in the calculations are reported in Table I. The optical parameters of Ref. 16 have been obtained by infrared reflectivity, which is an optical technique more sensitive to the bulk, while we are dealing here with a surface-sensitive technique. The good agreement between the theoretical spectrum deduced from these optical parameters and the HREELS spectrum demonstrates that the interdiffusion-assisted MBE process used here can produce good-quality AlSb crystalline films as thick as 1000 Å with low defect density.

The parameters listed in Table I allow us to calculate the dielectric response function of the AlSb/Sb heterostructure for arbitrary AlSb thickness through Eqs. (1)–(4). The EELS spectrum can then be computed fol-

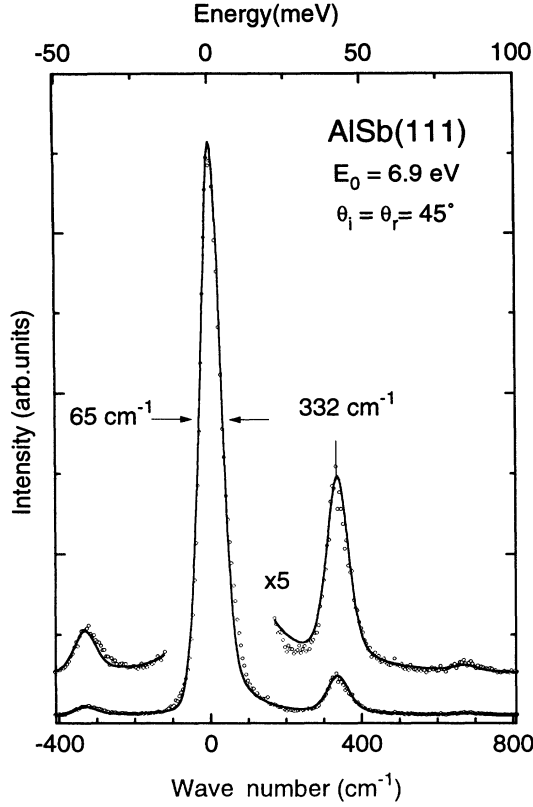


FIG. 3. HREELS spectrum recorded on a 1000-Å-thick AlSb layer grown on Sb. Superimposed on the experimental spectrum is the result of a dielectric theory calculation using the AlSb optical parameters of Table I.

lowing the procedure summarized above and described in detail in Ref. 17. The results of these calculations are shown by the full curves of Fig. 1, which we now analyze and compare with the experimental data.

A. Frequency analysis

In the frequency domain covered by HREELS, the dielectric function ϵ_b of the Sb substrate is very large in comparison to ϵ_s and, accordingly, Eq. (1) can be simplified in

$$\xi(\mathbf{q}_{\parallel}, \omega) = \frac{\epsilon_s(\omega)}{\tanh(q_{\parallel}d)}. \quad (5)$$

Within this approximation, the surface dielectric function [Eq. (4)] of the target system possesses one pole at a frequency ω_1 given by $\epsilon_s(\omega_1) = -\tanh(q_{\parallel}d)$, which corresponds to the well-known condition $\xi = -1$ for the existence of a surface mode. For a given wave vector q_{\parallel} , the frequency of this mode varies with the layer thickness d , from the AlSb LO frequency $\omega_{LO} = 334 \text{ cm}^{-1}$ for $d = 0$ to the frequency of the FK mode of the thick sample, $\omega_{FK} = 332 \text{ cm}^{-1}$ as $d \rightarrow \infty$. Due to the small oscillator strength, the overall dispersion of 2 cm^{-1} is too small to be measurable in our spectra. In agreement with the experimental data, one concludes that a single loss peak characterizes the HREELS spectra of AlSb/Sb, and the

frequency of this mode is close to the frequency of the FK phonon of AlSb, independent on the layer thickness.

B. Intensity analysis

The frequency behavior predicted by the two-layer model is consistent with the experimental observations and gives a degree of confidence in that description. In order to proceed deeper in the comparison, we now analyze the thickness dependence of the loss intensity of the surface optical phonon. In the dielectric theory applied to AlSb/Sb, the surface loss function $\text{Im}(g)$ deduced from Eqs. (4) and (5) when it is again assumed that $\epsilon_b \rightarrow \infty$ is written

$$\text{Im}(g) = \frac{\Omega_1^2}{\omega_1} \delta(\omega - \omega_1), \quad (6)$$

where ω_1 is the frequency of the surface mode introduced above. The oscillator strength Ω_1^2 for this mode is readily obtained in the form

$$\Omega_1^2 = \pi \tanh(q_{\parallel}d) \frac{\epsilon(0) - \epsilon(\infty)}{[\epsilon(\infty) + \tanh(q_{\parallel}d)]^2} \omega_{TO}^2. \quad (7)$$

Multiplying the oscillator strength by the kinematic factor of EELS and integrating over the wave vectors collected by the spectrometer¹⁷ yields the intensity of the

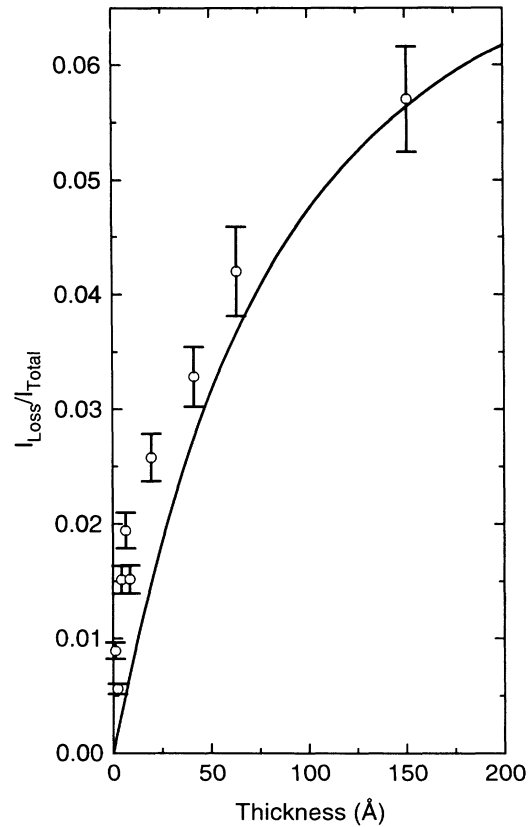


FIG. 4. Fuchs-Kliwer surface phonon of AlSb vs the aluminum coverage given as uniform AlSb layer thickness. The measured intensities are determined from the ratio between the loss peak area and the total spectrum area. The solid line is the result of a theoretical calculation using the dielectric theory.

loss peak plotted in Fig. 4 versus the layer thickness d . The temperature effects have been accounted for by multiplying the intensity of the loss peak by the Bose-Einstein factor¹⁷ $n(\omega_1) + 1 = \frac{1}{2}[\coth(\hbar\omega_1/2kT) + 1]$. For comparison, the experimental intensities are also shown in Fig. 4. These intensities have been determined as the ratio between the area under the loss peak and the total area under the HREELS spectra of Fig. 1. As it was already clear from Fig. 1, the loss intensities computed for small coverages are significantly smaller than the experimental ones. This discrepancy is mainly attributable to the uncertainty in the measurement of the coverage. Indeed, the Al flux was calibrated for a given cell temperature by measuring the average growth rate over a long period of time (typically 30 min to 1 h). This may result in an underestimation of the growth rate for very thin layers since, with the Al cells used here, the Al flux usually decreases slightly during the first few minutes of growth. Moreover, the use of the bulk dielectric function of AlSb for very thin films in the dielectric theory may lead to some additional unknown deviation.

The loss intensity of the AlSb surface phonon deduced from the theory behaves like $\tanh(q_{\parallel}d)$, where q_{\parallel} is a wave vector of the order of 0.01 \AA^{-1} , typical of the surface excitations in specular EELS. The experimental data shown in Fig. 4 reproduce this behavior remarkably well. Our simple model describes the surface phonon excitation in specular EELS for a perfect layer-by-layer growth of crystalline AlSb on Sb. The good agreement between this ideal case and the experimental data, taking into account the uncertainty in the measurement of the

layer thickness, allows us to conclude that the reactive growth of AlSb on top of the Sb single crystal proceeds nearly by a layer-by-layer mode.

CONCLUSION

We have studied by HREELS the reactive interface formation of elemental aluminum deposited at 600 K onto an antimony single crystal. At the earlier stage of the growth, a peak is clearly resolved at 332 cm^{-1} in the loss region of the spectrum. It is related to the excitation of an optical surface phonon and fingerprints the formation of crystalline AlSb as indicated by LEED. After several Al deposition steps, the surface loss peak does not present any significant shift in frequency allowing us to rule out the existence of intermediate bonding stages. The intensity of the loss peak is found to be strongly dependent on the Al coverage. The data are interpreted with the help of the dielectric theory using a two-layer model, which confirms a layer-by-layer growth mode for the reactive interface Al/Sb(111).

ACKNOWLEDGMENTS

Two of us (R.S. and Ph.L.) are grateful to the Belgian National Fund for Scientific Research for financial support. This work was partly funded by the Belgian national program of Interuniversity Research Projects initiated by the State Prime Minister Office (Science Policy Programming) and by the Belgian Fund for Joint Basic Research.

¹T. D. Golding, J. A. Dura, W. C. Wang, J. T. Zorobowski, D. C. Chen, Z. Zou, J. H. Miller, and J. R. Meyer (unpublished).

²R. Sporcken, P. A. Thiry, E. Petit, J. J. Pireaux, R. Caudano, J. Ghijsen, R. L. Johnson, and L. Ley, *Phys. Rev. B* **35**, 7927 (1987).

³R. Sporcken, P. Xhonneux, R. Caudano, and J. P. Delrue, *J. Vac. Sci. Technol. A* **6**, 1565 (1988).

⁴R. Fuchs and K. L. Kliewer, *Phys. Rev.* **140**, 2076 (1965).

⁵H. Ibach, *Phys. Rev. Lett.* **24**, 1416 (1970).

⁶P. A. Thiry, M. Liehr, J. J. Pireaux, and R. Caudano, *Phys. Rev. B* **29**, 824 (1984).

⁷R. Matz and H. Lüth, *Phys. Rev. Lett.* **46**, 500 (1981).

⁸P. A. Thiry, M. Liehr, J.-J. Pireaux, R. Caudano, and T. Kuech, *J. Vac. Sci. Technol.* **4**, 953 (1986); J.-L. Guyaux, P. A. Thiry, R. Sporcken, Ph. Lambin, and R. Caudano, *Phys. Rev. B* **48**, 4380 (1993).

⁹L. H. Dubois and G. P. Schwartz, *Phys. Rev. B* **26**, 794 (1982).

¹⁰A. Ritz and H. Lüth, *Phys. Rev. Lett.* **52**, 1242 (1984).

¹¹P. A. Thiry, J.-L. Longueville, J.-J. Pireaux, and R. Caudano, *J. Vac. Sci. Technol.* **5**, 603 (1986).

¹²R. Sporcken, P. Louette, J. Gérard, R. Caudano, and J.-P. Delrue, *Fresenius Z. Anal. Chem.* **329**, 370 (1987).

¹³J.-L. Guyaux, R. Sporcken, R. Caudano, V. Wagner, J. Geurts, and W. Richter (unpublished).

¹⁴H. Ibach and D. L. Mills, *Electron Energy Loss Spectroscopy and Surface Vibrations* (Academic, New York, 1982).

¹⁵A. A. Lucas, J.-P. Vigneron, Ph. Lambin, P. A. Thiry, M. Liehr, J.-J. Pireaux, and R. Caudano, *Int. J. Quantum Chem.* **19**, 687 (1986).

¹⁶W. J. Turner and W. E. Reese, *Phys. Rev.* **127**, 126 (1962).

¹⁷Ph. Lambin, J.-P. Vigneron, and A. A. Lucas, *Comp. Phys. Commun.* **60**, 351 (1990).